steel research international
www.steel-research.de

Thermal and Thermomechanical Responses Prediction of a Steel Ladle Using a Back-Propagation Artificial Neural Network Combining Multiple Orthogonal Arrays

Aidong Hou, Shengli Jin, Harald Harmuth, and Dietmar Gruber*

To facilitate industrial vessel lining design for various material properties and lining configurations, a method, being composed of the back-propagation artificial neural network (BP-ANN) with multiple orthogonal arrays, is developed, and a steel ladle from secondary steel metallurgy is chosen for a case study. Ten geometrical and material property variations of this steel ladle lining are selected as inputs for the BP-ANN model. A total of 160 lining configurations nearly evenly distributed within the ten variations space are designed for finite element (FE) simulations in terms of five orthogonal arrays. Leave-One-Out cross validation within various combinations of orthogonal arrays determines 7 nodes in the hidden layer, a minimum ratio of 16 between dataset size and number of input nodes, and a Bayesian regularization training algorithm as the optimal definitions for the BP-ANN model. The thermal and thermomechanical responses of two optimal lining concepts from a previous study using the Taguchi method are predicted with acceptable accuracy.

1. Introduction

Steel ladles, which consist of refractories and steel construction components, act as transportation vessels and refining units in the steelmaking industry. Refractory linings protect steel shells from steel melt, and reduce heat loss from the steel shells. A well-lined steel ladle offers efficient temperature control of the steel melt, and is beneficial to the steel quality and productivity.[1–4]

The performance of a steel ladle is influenced by many factors; for instance, material properties, lining thicknesses, and process conditions. Efforts have been made to evaluate the performance of steel ladle linings from thermal and thermomechanical viewpoints using finite element (FE) methods, especially taking into account the application of insulation and preheating time.[5–10] Integrated consideration of lining concepts for a steel ladle is also of importance to support steel industry 4.0 in refractory application.[11,12] Recently, the authors applied the Taguchi method to optimize lining design configurations with FE simulations within a defined variable span of lining thickness and material properties.[5] The impact of factors on the thermal and thermomechanical responses was quantitatively assessed using the analysis of variance and signal-to-noise ratio. Finally, two optimal lining concepts were proposed, which showed a substantial decrease in heat loss through the cylindrical steel shell and the thermomechanical load at the hot face of the working lining. This approach offers a primary tool to assess the significance of variables and select the optimal lining concept among the defined values of variables. Nevertheless, the instantaneous prediction of thermal and thermomechanical results of several proposed lining concepts after assessment is also desirable for efficient design of lining concepts, which are included in the defined span, but were fully or partly excluded from the defined values in the dataset used for training.

The artificial neural network (ANN) provides a promising technique to fulfil this target, and is one of the most extensively used methods in prediction based artificial intelligence and machine learning.[13] It can be categorized as feed forward or recurrent. In contrast to recurrent neural networks, a feed forward neural network processes information from the input nodes, through the hidden nodes to the output nodes, without the information transfer process among the hidden nodes.[14] Multilayer perception is usually preferable in feed forward neural networks trained with different error-back propagation (BP) algorithms.[15] This type of ANNs has advantageous characteristics; for instance, generalization, adaptation, and robustness.[16] It is successfully applied in materials engineering to predict the mechanical properties of materials,[17–19] lifetime limited by fatigue crack propagation, and chemical compositions of alloys.[15,20]

The predictive quality of an ANN model depends on the quality of the dataset, and on the architectural parameters, including the number of hidden layers and nodes per layer, and the training algorithms.[21] It is important to collect data in a way that ensures they are representative in the entire variable space

A. Hou, Dr. S. Jin, Prof. H. Harmuth, Dr. D. Gruber
Chair of Ceramics
Montanuniversitaet Leoben
A-8700 Leoben, Austria
E-mail: shengli.jin@unileoben.ac.at

The ORCID identification number(s) for the author(s) of this article can be found under https://doi.org/10.1002/srin.201900116.

DOI: 10.1002/srin.201900116

with low influence from noise; the minimum size of a training dataset largely depends on the complexity of the problem and applied ANN architectures.[21] The minimum dataset size is approximately proportional to the total number of free parameters divided by the fraction of errors permitted.[22] For instance, with an error allowance of 10%, the training dataset size shall be about 10 times the number of weights and biases in the network. For complex models, the minimum size of a training dataset may deviate from this rule.[23]

The numbers of hidden layers and nodes in each layer are significant parameters affecting the performance of an ANN model. With a larger number of hidden layers or nodes, an ANN model can yield more accurate training results and is able to model more complicated relationships, while it also increases the risk of over-fitting. In contrast, with a smaller number of hidden layers or nodes, an ANN model may be insufficient to depict the underlying relationships.[24] Several empirical equations are proposed to define the node number in a hidden layer.[25]

$$N_{\text{out}} < N_{\text{hid}} < N_{\text{inp}} \tag{1}$$

$$N_{\text{hid}} \approx 2/3\ N_{\text{inp}} + N_{\text{out}} \tag{2}$$

$$N_{\text{hid}} \leq 2\ N_{\text{inp}} \tag{3}$$

where N_{inp}, N_{hid}, and N_{out} are the node number of an input layer, hidden layer, and output layer, respectively.

The training algorithm for the back-propagation procedure also affects the performance of an ANN model. It is used to tune the weights in the network so that the network performs a suitable mapping process from inputs to outputs.[24] The error function (E) represents a measure of network performance; E is defined as the mean square error between the outputs from network and the target values:

$$E = \frac{1}{N_t}\sum\nolimits_{i=1}^{N_t} (d_i - y_i)^2 \tag{4}$$

where N_t is the total number of training samples, i is the sample index, $\mathrm{d_i}$ is the actual value of the $\mathrm{i^{th}}$ training sample, and y_i the predicted value of the $\mathrm{i^{th}}$ training sample.

Many training algorithms have been developed to minimize the error function with different strategies.[26–28] For instance, gradient descent algorithms offer the possibility to define learning rate and momentum for the steepest descent during back-propagation. In contrast with gradient descent algorithms, conjugate gradient algorithms utilize the previous gradient search direction to define the present one; quasi-Newton algorithms use a Hessian matrix to define the descent direction; the Bayesian regularization algorithm minimizes the linear combination of squared errors and weights by applying the Levenberg-Marquardt algorithm. To identify which training algorithm is better is non-trivial; nevertheless, a good training algorithm should show acceptable robustness, computational efficiency, and generalization ability.

The present work aimed to develop a methodology for applying a reliable back-propagation (BP) ANN model to predict the thermal and thermomechanical responses of a steel ladle within a defined variable space. Multiple orthogonal arrays were employed to generate lining configurations for FE simulations and BP-ANN model training. The sufficiency of the dataset, feasible node number in the hidden layer for a case study with 10 variables, and the training algorithms were investigated. Later, a BP-ANN model with optimized settings was applied to predict the results of two lining concepts proposed in the Hou et al.[5]

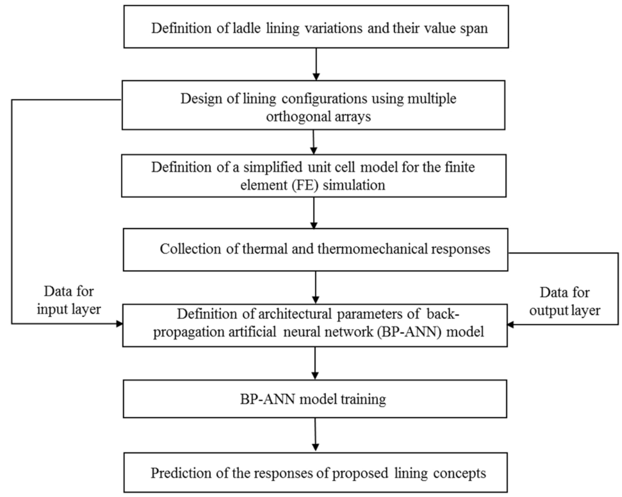

Figure 1. Flowchart of a methodology to predict thermal and thermomechanical responses of a steel ladle.

2. Methodology

A flowchart of this methodology for predicting the thermal and thermomechanical responses of a steel ladle is illustrated in **Figure 1**, and includes lining configuration design, FE modeling, and BP-ANN model training and prediction.

2.1. Finite Element Model and Boundary Conditions

Figure 2 depicts a simplified two-dimensional model representing a horizontal cut through the slag-line position in the upper part of the steel ladle. The outer diameter of the steel ladle was 1.828 m for all of the established models. The model consists of a two-half brick working and permanent lining, an insulation lining, a fiberboard, and a steel shell. The circumferential expansion allowance between bricks was 0.4 mm. Variations were lining and steel shell thicknesses, thermal conductivity, and Young's modulus of lining materials.

FE-modeling of the steel ladle, taking into account elastic material behavior, was performed using the commercial code

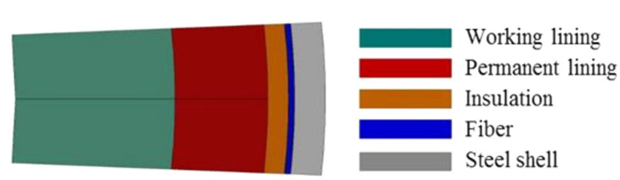

Figure 2. Finite element (FE) model geometry.

Abaqus. The simulation included the preheating of the working lining hot face to 1100 °C over 20 h, and a subsequent thermal shock caused by tapping the steel melt of 1600 °C into the ladle. After a refining period of 95 min proceeded a 50 min idle period. Displacement of linings was allowed in the radial direction and constrained in the circumferential direction with a symmetry condition. The heat transfer between the liquid melt and hot face of the working lining, the cold end of the steel shell, and the atmosphere was defined as being temperature-dependent using the surface film condition function (**Table 1**) in Abaqus. The interfaces between linings were crossed by heat flux, and a heat transfer coefficient allowing for radiation and convection was applied.

2.2. Sample Screening Approach

Orthogonal arrays are highly fractional factorial designs that yield a minimum number of experimental runs. With orthogonal array design, the combination of each level of two or more variables occurs with equal frequency.[29]

Multiple orthogonal arrays were applied to arrange the level combination of the ten factors within various defined variable spaces. The definition of values in the respective span of a variable in each orthogonal array was arbitrary, and an even distribution of the values in the maximum span was designed. Detailed variations and the associated intervals are listed in **Table 2**. Nine of the studied factors had four levels, and the thickness of the steel shell had two levels. A total of 5 variable spaces were defined; thus, 5 mixed-level orthogonal arrays L32 ($4^9 \times 2^1$) with 32 runs were implemented accordingly, which yielded the total dataset size of lining configurations equal to 160. The lining configurations according to the orthogonal array containing the maximum or minimum level value constituted the boundary space, termed space A, and were used only for BP-ANN model training. The lining configurations from the other four orthogonal arrays were named as spaces B, C, D, and E. The maximum level values of all 10 factors in spaces B, C, D, and E were defined in a descending order, and their minimum level values were in an ascending order accordingly. Spaces B-E were used for BP-ANN model training and testing.

Table 1. Film coefficient (W m^{-2} K^{-1}) defined in the finite element (FE) model.

Temperature (°C)	Hot face of working lining	Temperature (°C)	Cold end of steel shell
10	10	10	10
150	60.1	50	10
250	99	150	15
350	149.9	250	21
400	181.1	350	27
650	409.5	400	32
700	472.3	650	50
800	617.8	700	70
1000	998.5	1000	140
1200	1517	1600	400
1600	3052.3	2000	400

2.3. BP-ANN Model Establishment and Parameter Study Design

The BP-ANN model was made of three layers with various nodes: one input layer, one hidden layer, and one output layer. Nodes in the former layer were connected to each node in the latter layer, as shown in **Figure 3**. Input variables (X) were introduced to the network as a vector corresponding to the nodes in the input layer. These input variables were multiplied by their respective weights (W) and plused a bias (b) constant, yielding a summation (S) for each node of the hidden layer, as shown in Equation (5). An activation function was used to limit the amplitude of the summation of each hidden layer node, which is the input for the output layer nodes, as depicted by Equation (6). A hyperbolic tangent sigmoid activation function (tansig) was applied as shown in Equation (7).

$$S_k = \sum_{j=1}^{N_{inp}} W_{jk} X_j + b \tag{5}$$

$$O_k = f(S_k) \tag{6}$$

$$f_{\text{tansig}} = \frac{1 - e^{-2S_k}}{1 + e^{-2S_k}} \tag{7}$$

where j is the input factor index, k is the node index in the hidden layer, S_k is the summation at the k^{th} node in the hidden layer, f is the activation function, W_{jk} is the weight of the j^{th} input at the k^{th} node, X_j is the j^{th} input, b is the bias, and O_k is the output of the k^{th} node in the hidden layer. The information transfer

Table 2. Geometrical and material property variations for the selected ladle.

	Ladle linings	Range of variable values	Label of factors
Thickness (m)	Working lining	0.03–0.27	X_1
	Permanent lining	0.05–0.14	X_2
	Insulation	0.003–0.042	X_3
	Steel shell	0.015–0.035	X_4
Thermal conductivity (Wm^{-1}K^{-1})	Working lining	1.5–10.5	X_5
	Permanent lining	1.0–10.0	X_6
	Insulation	0.05–1.55	X_7
Young's modulus (GPa)	Working lining	25–115	X_8
	Permanent lining	5–110	X_9
	Insulation	0.1–39.1	X_{10}

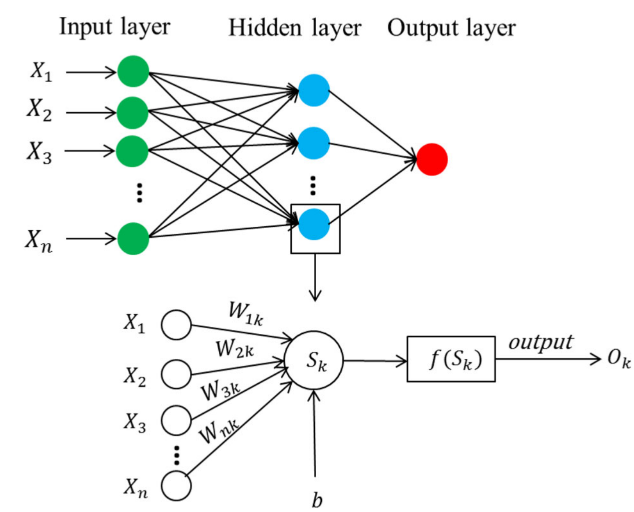

Figure 3. Topology of a three-layer artificial neural network.

between the hidden layer and output layer followed the same mathematical process, and in the present paper a linear activation function (purelin) was applied:

$$f_{\text{purelin}} = S_m \tag{8}$$

where m is the node index in the output layer, and S_m is the summation at the m^{th} node in the output layer.

Before ANN training starts, the input variables of the network must be defined. When the ranges and units of input variables are different from each other, it is wise to normalize input data to mitigate the influence of magnitudes. In the present study, input variables were normalized (X_i) to a scale of 0.1–0.9 using the following equation for a variable x:

$$X_i = \frac{0.1x_{\max} - 0.9x_{\min} + 0.8x_i}{x_{\max} - x_{\min}} \tag{9}$$

where $x_{\max}$ and $x_{\min}$ represent the maximum and minimum of the variable x.

To determine the optimal BP-ANN architectural parameters for thermal and thermomechanical responses, three tests were carried out with temperature response and parameters optimized sequentially. Afterwards, thermomechanical responses were used to test the generality of the established BP-ANN model. Training was terminated by reaching any defined criterion; for instance, the minimum performance gradient (10^{-5}), the minimum target error (0), or a maximum number of epochs (one epoch includes one forward pass and one backward pass of all the training samples, 10 000 as default value if there is no explicit definition).

First, a test was performed to explore the optimal node number in the hidden layer. All 160 samples were used for BP-ANN training, and the training algorithm was a gradient descent with momentum and adaptive learning rate back-propagation (GDX; **Table 3**). The number of nodes in the hidden layer varied from 1 to 12. The objective of the second test was to identify the minimum sample size for the lining concept study. The dataset was divided into three groups, which contained 96, 128, and 160 samples. All three groups included 32 samples in boundary space A. The residual samples in each group were the combination of any two, three, and four variable spaces except boundary space A. Eight training algorithms (Table 3) in the Deep Learning Toolbox of Matlab[30] were employed individually in the third test to detect the training algorithm most favorable for the steel ladle. A summary of these three tests is listed in **Table 4**.

Table 3. Training algorithms employed in this study.[30]

Training algorithm	Brief description
GDX	Gradient descent with momentum and adaptive learning rate back-propagation
CGB	Conjugate gradient back-propagation with Powell-Beale restarts
CGF	Conjugate gradient back-propagation with Fletcher-Reeves updates
CGP	Conjugate gradient back-propagation with Polak-Ribiére updates
SCG	Scaled conjugate gradient back-propagation
BFG	BFGS quasi-Newton back-propagation
OSS	One-step secant back-propagation
BR	Bayesian regularization back-propagation

Leave-one-out (LOO) cross validation and figures of merit were employed in these three tests to quantitatively assess the performance of the established BP-ANN model. LOO applies one sample for prediction and the residual samples of the entire dataset for training. Four quantities were used: maximum relative error (RE_MAX), mean relative error (MRE), relative root mean squared error (RRMSE), and coefficient of determination (B), as shown in Equations (10)–(13):

Maximum relative error of all testing samples:

$$\text{REMAX} = \text{Max}\left(\frac{|d_i - y_i|}{d_i}\right) \tag{10}$$

$$\text{Mean relative error : MRE} = \frac{1}{n}\sum\nolimits_{i=1}^{n} \frac{|d_i - y_i|}{d_i} \tag{11}$$

Relative root mean squared error:

$$\text{RRMSE} = \frac{\sqrt{\frac{1}{n}\sum\nolimits_{n}^{i=1} (d_i - y_i)^2}}{\bar{d}} \tag{12}$$

Table 4. Tests for the design of BP-ANN model architectural parameters.

Test	Architectural factors of BP-ANN model	Testing parameters
1	The number of nodes in hidden layer	12 (from 1 to 12)
2	Dataset size	3 groups (96, 128, and 160 samples)
3	Training algorithms	8 (GDX, CGB, CGF, CGP, SCG, BFG, OSS, BR; available in Matlab)

$$\text{Coefficient of determination}: B = 1 - \frac{\sum_{n}^{i=1}(d_i - y_i)^2}{\sum_{n}^{i=1}(d_i - \bar{d})^2} \qquad (13)$$

where n is the number of testing samples, y_i is the predicted value of the ith testing sample by the BP-ANN model with LOO, d_i is the response value of the ith testing sample from FE modeling, and $\bar{d}$ is the mean response value of all testing samples received from the FE modeling.

3. Results and Discussion

3.1. Node Number in the Hidden Layer

The BP-ANN model predicts the temperatures at the steel shell at the end of the idle period with various numbers of nodes in the hidden layer with epochs of 1000. Low values of RE_MAX, MRE, and RRMSE, and a larger value of B are desirable. Dimensionless calculation was performed for each quantity relative to its largest value. As shown in **Figure 4**, the node number in the hidden layer affects BP-ANN performance in a complex manner. Generally speaking, cases with node numbers of 4-7 and 9 showed satisfying results. Although the case with the node number 7 showed slightly higher RE_MAX, its MRE and RRMSE were the minima among the 12 cases.

Therefore, for an input layer with 10 nodes, node number 7 of the hidden layer was proposed for the further study. This result was consistent with a previously stated rule,[25] which defines that the node number of the hidden layer shall be approximately equal to two thirds of the node number in the input layer plus the node number in the output layer, as stated in Equation (2). In the present study, this rule yielded 7.67.

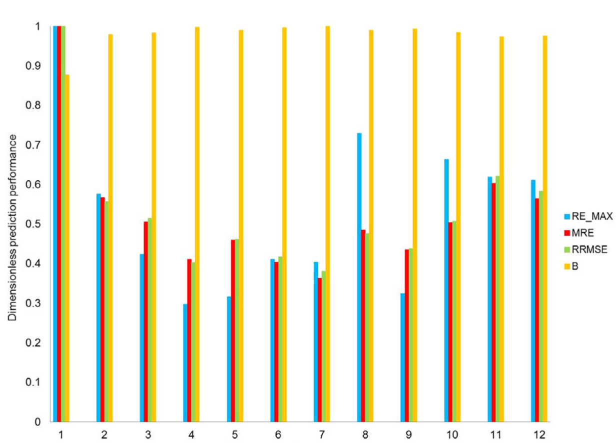

Figure 4. Performance assessment of the back-propagation artificial neural network (BP-ANN) model for temperature prediction with different node numbers in the hidden layer and by applying the GDX (gradient descent with momentum and adaptive learning rate back-propagation) training algorithm.

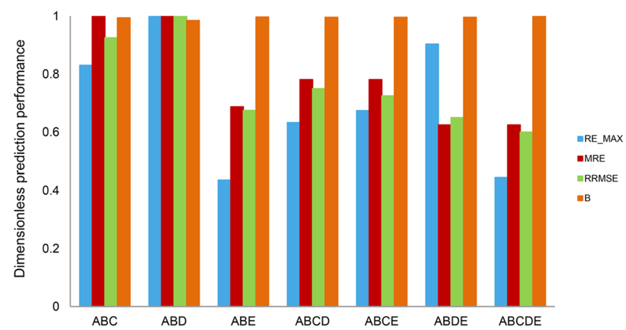

Figure 5. Performance assessment of the back-propagation artificial neural network (BP-ANN) model for temperature prediction with different dataset sizes and by applying the GDX (gradient descent with momentum and adaptive learning rate back-propagation) training algorithm.

3.2. Dataset Size

Seven cases with different combinations of orthogonal arrays were defined to test the appropriate dataset size for reliable BP-ANN models to predict the temperature response. The dataset size of ABC, ABD, and ABE is 96; that of ABCD, ABCE, and ABDE is 128, and that of ABCDE is 160. The dimensionless performance of BP-ANN models for the seven cases is represented in **Figure 5**. In general, better performance was achieved by increasing the dataset size. The BP-ANN model with

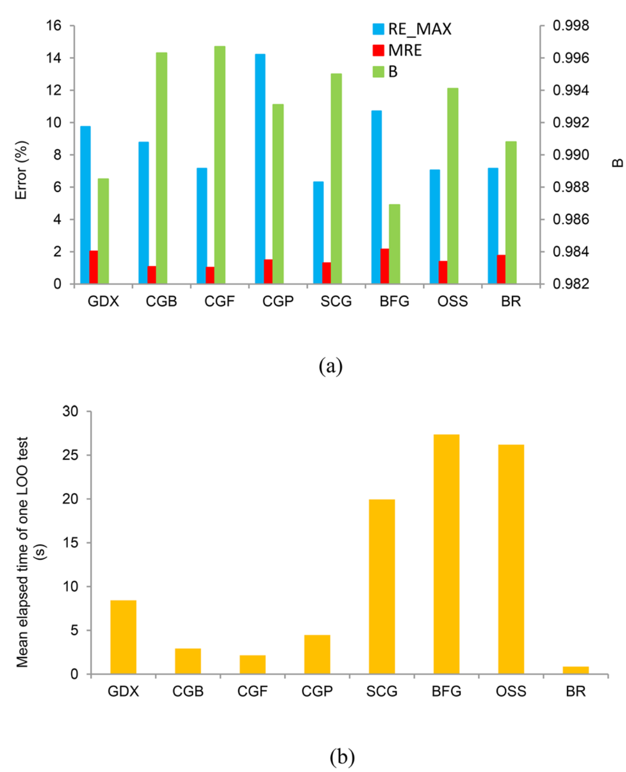

Figure 6. Performance assessment of the back-propagation artificial neural network (BP-ANN) model for (a) temperature prediction based errors, and (b) computation time with different training algorithms.

Table 5. Thermomechanical responses prediction performance of BP-ANN models with CGF and BR.

Criteria	End temperature		Maximum tensile stress		Maximum compressive stress	
	CGF	BR	CGF	BR	CGF	BR
RE_MAX (%)	7.15	7.15	16.62	12.43	3.12	4.09
MRE (%)	1.02	1.76	2.43	2.37	0.93	0.78
B	0.9967	0.9908	0.9279	0.9348	0.9963	0.9966
Mean elapsed time of one LOO test (s)	2.15	0.86	3.16	1.12	1.38	0.68

96 samples from spaces of A, B, and E showed good prediction performance; Given the worse performance was of ABC and ABD, a conservative minimum sample size for the present study was 160, which is 16 times the number of inputs.

3.3. Training Algorithms

Eight training algorithms to predict end temperature at the cold end of the steel shell were employed individually in order to train the BP-ANN model with the above determined architectural parameters. Besides RE_MAX, MRE, and B, the mean elapsed time for training 159 samples and prediction of one sample in LOO tests was additionally applied to evaluate the efficiency of the model. The performance results are presented in **Figure 6**. Lower error values, larger B, and shorter computation time are favorable. As shown in Figure 6a, the RE_MAX and MRE from the cases with algorithms CGF, SCG, OSS, and BR were less than those from GDX, CGB, CGP, and BFG, and showed acceptable coefficients of determination. However, calculations with algorithms SCG and OSS were time consuming (Figure 6b). Therefore, the algorithms CGF and BR were proposed for further study.

3.4. Extension to Thermomechanical Response Study

To finalize the model infrastructure, the above-determined BP-ANN model with 7 nodes in the hidden layer and 160 samples in the dataset was trained, using both CGF and BR, to predict thermomechanical responses. **Table 5** summaries the prediction performance comparison of algorithms CGF and BR in thermal and thermomechanical responses. The BP-ANN model trained using BR performed better than the model with CGF for the maximum tensile stress and compressive stress. Therefore, a BP-ANN model with BR was proposed for the steel ladle study.

It is noteworthy that the prediction performance of this BP-ANN model with BR for maximum tensile stress is inferior to that for end temperature and maximum compressive stress. A previous study[5] showed that 7 of the 10 defined factors contribute 91% to the maximum tensile stress, followed by 5 factors contributing 94% to the end temperature, and 1 factor contributing 93% to the maximum compressive stress. The high dimensionality occurring in the factor-response space increases the complexity of the problem and results in under-fitting. Conversely, if the maximum tensile stress prediction was used for parameter study, one could expect over-fitting of the end temperature and maximum compressive stress. An alternative could be establishing the BP-ANN models with regard to the individual response, instead of the three responses. Nevertheless, the RE_MAX for the maximum tensile stress was 12.43%, which is less than the 15% empirical error tolerance of prediction.[19,31,32] Moreover, the MSE was as low as 2.37%; therefore, the BP-ANN model was sufficient for the research requirements.

3.5. Prediction with the Optimized BP-ANN Model

The optimal configuration of the BP-ANN model contains 7 nodes in the hidden layer, and applies the Bayesian regularization method, with 160 samples for training. The configurations and the results of the comparison of predicted values for two proposed lining concepts are given in **Table 6** and **Table 7**, respectively. The temperature difference between the BP-ANN model and the FE results was 4 K for lining concept 1, and the BP-ANN model predicted the same temperature as the FE modeling of lining concept 2. The maximum tensile stress differences between BP-ANN prediction and FE modeling for the two lining concepts were 62 and 37 MPa, representing 4.1% and 2.4%, respectively. The differences in maximum compressive stress between BP-ANN prediction and FE modeling for the two lining concepts were 5 and 2 MPa, representing 0.97% and 0.39%, respectively.

Table 6. Two proposed optimal lining concepts with different insulation materials. [5]

	Thickness (mm)	Thermal conductivity ($W\ m^{-1}K^{-1}$)	Young's modulus (GPa)	Thermal expansion coefficient ($10^{-6}K^{-1}$)
Working lining	155	9	40	12.0
Permanent lining	52.5	2.2	45	5.0
Insulation (Lining concept 1)	37.5	0.5	3	6.0
Insulation (Lining concept 2)	37.5	0.38	4	5.6
Steel shell	30	50	210	12.0

Table 7. Comparison of simulated and predicted values of two proposed optimal lining concepts from FE modeling and BP-ANN.

	Steel shell temperature (°C)		Maximum tensile stress (MPa)		Maximum compressive stress (MPa)	
	FE modeling	Prediction	FE modeling	Prediction	FE modeling	Prediction
Lining concept 1	280	276	1495	1433	512	517
Lining concept 2	259	259	1539	1576	517	515

4. Conclusion and Outlook

A BP-ANN model was developed to predict the thermal and thermomechanical responses of a steel ladle considering 10 geometrical and material property variations of ladle linings. The optimized architectural parameters of the proposed BP-ANN model were 7 nodes in the hidden layer, a dataset size not less than 16 times the number of input nodes, and a Bayesian regularization training algorithm. The LOO tests for 128 samples showed that the coefficient of determination of the end temperature, the maximum tensile stress at the steel shell, and the maximum compressive stress at the hot face of the working lining were high. The proposed BP-ANN model was further utilized to predict the responses of two lining configurations proposed by previous work, and the high prediction accuracy confirmed the reliable performance of the BP-ANN model.

As an alternative to the conventional trial-and-error method, the numerical investigation of lining concepts for a given industrial vessel can be beneficial in saving time, materials, and labor by avoiding unnecessary industrial trials. On the other hand, the BP-ANN method allows an efficient search for optimized lining concepts for vessels from both energy savings and better thermomechanical performance points of view.

The proposed multiple orthogonal arrays and BP-ANN methods developed in the present paper are also promising for the optimization of ironmaking and steelmaking processes and material recipe development. Especially, the application of multiple orthogonal arrays is an advanced tool to achieve a representative variations-response space, which defines the establishment of BP-ANN model and affects the prediction performance.

Acknowledgements

The Competence Center for Excellent Technologies research programme in "Advanced Metallurgical and Environmental Process Development" (K1-MET) is supported by the Austrian Competence Centre Programme COMET (Competence Center for Excellent Technologies) with funds from the Federal Ministry for Transport, Innovation and Technology, the Federal Ministry of Economy, the provinces of Upper Austria and Styria, the Styrian Business Promotion Agency, and the Tyrolian Future Foundation.

Conflict of Interest

The authors declare no conflict of interest.

Keywords

artificial neural network, back-propagation, orthogonal array, lining concept, steel ladle, thermomechanical responses

Received: March 4, 2019
Revised: April 2, 2019
Published online:

[1] A. Ghosh, *Secondary Steelmaking: Principles and Applications*, CRC Press, Florida, USA, **2000**.
[2] A. Zimmer, A. N. C. Lima, R. M. Trommer, S. R. Braganca, C. P. Bergmann, *J. Iron. Steel. Res. Int.* **2008**, *15*, 11.
[3] O. Volkova, D. Janke, *ISIJ Int.* **2003**, *43*, 1185.
[4] C. E. Baukal Jr, *Industrial Combustion Pollution and Control*, CRC Press, New York, USA **2003**.
[5] A. Hou, S. Jin, H. Harmuth, D. Gruber, *JOM*. **2018**, *70*, 2449.
[6] D. Gruber, H. Harmuth, *Steel. Res. Int.* **2008**, *79*, 913.
[7] G. Li, J. Liu, G. Jiang, H. Liu, *Adv. Mech. Eng.* **2015**, *7*, 1.
[8] D. Gruber, T. Auer, H. Harmuth, *Rotsch J, in Steelsim 2007*, TIB, Graz, Austria **2007**, p. 291.
[9] D. Gruber, H. Harmuth, *Steel. Res. Int.* **2014**, *85*, 512.
[10] S. Jin, T. Auer, D. Gruber, H. Harmut, M. H. Frechette, Y. Li, *Interceram/Refractories Manual*. **2012**, 37.
[11] S. Jin, D. Gruber, H. Harmuth, J. Soudier, P. Meunier, H. Lemaistre, *Int. J. Cast. Met. Res.* **2014**, *27*, 336.
[12] S. Jin, H. Harmuth, D. Gruber, Proc. 60th Int Colloq Refract, TIB, Aachen, Germany, **2017**, p. 66.
[13] A. Alibakshi, *Anal. Chim. Acta*. **2018**, *1026*, 69.
[14] L. Fausett, *Fundamentals of Neural Networks: Architecture, Algorithms, and Applications*, Prentice Hall, NJ, USA **1994**.
[15] J. R. Mohanty, B. B. Verma, D. R. K. Parhi, P. K. Ray, *Arch. Comput. Mat. Sci. Surface Eng.* **2009**, *01*, 133.
[16] J. M. O. Rodriguez, M. R. M. Blanco, J. M. C. Viramontes, H. R. V. Carrillo, in Artificial Neural Networks – Architectures and Applications, (Ed: K. Suzuki), InTech, Croatia **2013**, Ch. 4.
[17] S. H. Sadati, J. A. Kaklar, R. Ghajar, in Artificial Neural networks – Industrial and Control Engineering Applications, (Ed: K. Suzuki), InTech, Croatia **2010**, Ch. 5.
[18] J. Ghaisari, H. Jannesari, M. Vatani, *Adv. Eng. Softw.* **2012**, *45*, 91.
[19] C. Bilim, C. D. Atis, H. Tanyildizi, O. Karahan, *Adv. Eng. Softw.* **2009**, *40*, 334.
[20] Y. Sun, W. D. Zeng, Y. F. Han, X. Ma, Y. Q. Zhao, *Comput. Mater. Sci.* **2011**, *50*, 1064.
[21] L. A. Dobrzański, J. Trzaska and A. D. Dobrzańska-Danikiewicz, in Comprehensive Materials Processing, Vol. 2, (Eds: S. Hashmi, G. F. Batalha, C. J. Van Tyne, B. Yilbas), Elsevier, CO, USA **2014**, Ch. 9.
[22] S. Haykin, Neural Networks and Learning Machines, Pearson Education, Ontario, Canada **2009**.
[23] A. Alwosheel, S. Cranenburgh, C. G. Chorus, *J. Choice Model.* **2018**, *28*, 167.
[24] A. Radi, S. K. Hindawi, in Artificial Neural Networks – Architectures and Applications, (Ed: K. Suzuki), InTech, Croatia **2013**, Ch. 9.
[25] S. Karsoliya, *IJETT.* **2012**, *31*, 714.
[26] M. Moreira, E. Fiesler, IDIAP Technical Report, Martigny, Swizerland **1995**.

[27] Z. Cömert, A. F. Kocamaz, Bitlis. Eren. Univ. J. Sci. & Technol. **2017**, *7*, 93.
[28] M. Fernandez, J. Caballero, in Artificial Neural Network for Drug Design, Delivery and Disposition, (Eds: M. Puri, Y. Pathak, V. K. Sutariya, S. Tipparaju, W. Moreno), Academic Press, **2016**, Ch. 4.
[29] R. K. Roy, A Primer on the Taguchi Method, Society of Manufacturing Engineers, USA **2010**.
[30] MathWorks. Deep Learning Toolbox: User's Guide (R2018b).
[31] Z. Yuan, L. N. Wang, X. Ji, *Adv. Eng. Softw.* **2014**, *67*, 156.
[32] J. L. G. Rosa, in Artificial Neural Networks – Architectures and Applications, (Ed: K. Suzuki), InTech, Croatia **2013**, Ch. 2.